Supporting Information

*Jinyan Chen[1], Shouyi Sun[1, 2], Bin Zhang[3], Xinchun Chen[1], Jianbin Luo[1], Jinjin Li[*1]*

1 State Key Laboratory of Tribology in Advanced Equipment, Tsinghua University, Beijing 100084, PR China.

2 Department of Engineering Mechanics, Northwestern Polytechnical University (Chang' an Campus), Xi' an 710129, PR China

3 State Key Laboratory of Solid Lubrication, Lanzhou Institute of Chemical Physics, Chinese Academy of Sciences, Lanzhou 730000, China

Corresponding author:

*To whom all correspondence should be addressed.

Jinjin Li

Telephone: 8610-62797178

E-mail: lijinjin@mail.tsinghua.edu.cn

1. Deposition process and parameters of the coating

The a-C:H:Si films were deposited by middle-frequency magnetron sputtering in a mixed Ar/SiH_4 atmosphere. Prior to deposition, the chamber was evacuated to a base pressure of 5.0×10^{-3} Pa. During film growth, a graphite target (99.99% purity) was powered by a middle-frequency power supply (40 kHz) operated at a constant current of 10 A, corresponding to a target voltage in the range of 580–660 V. A negative substrate bias of −60 V with a duty ratio of 65% was applied throughout deposition. The working gases consisted of Ar (700 sccm) and SiH_4 (100 sccm). All films used in this work were deposited for a total duration of 120 min, resulting in a film thickness of approximately 0.95 μm, corresponding to a deposition rate of 7.9 nm/min.

N-type Si (100) wafers were used as substrates and were subjected to a multistep ultrasonic cleaning process prior to deposition. No additional metallic or silicon adhesion interlayer was introduced between the substrate and the a-C:H:Si film. A summary of the deposition parameters is provided in **Table S1**. Unless otherwise stated, all results presented in this work were obtained from films deposited at 100 sccm SiH_4, yielding a thickness of approximately 0.95 μm and a Si content of 4.37 at%.

Table S1. Deposition parameters of a-C:H:Si films

Parameter	Value
Deposition method	Middle-frequency magnetron sputtering
Target material	Graphite (99.99% purity)
Power supply frequency	40 kHz

Target current	10 A
Target voltage	580–660 V
Base pressure	5.0×10^{-3} Pa
Substrate bias voltage	−60 V
Bias duty ratio	65%
Working gases	Ar / SiH_4
Ar flow rate	700 sccm
SiH_4 flow rate	100 sccm
Substrate	N-type Si (100)
Substrate cleaning	Multistep ultrasonic cleaning
Adhesion interlayer	None
Deposition rate	7.9 nm/min

2. Pictures of friction test equipment

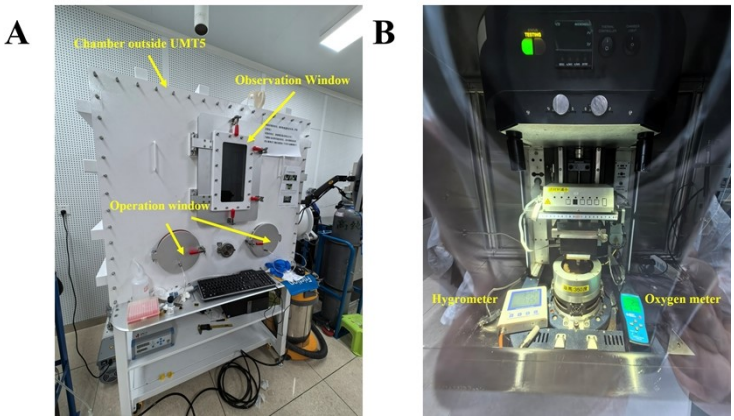

Figure S1. (A) Chamber outside UMT-5. (B) Friction test under high temperature in dry nitrogen.

3. Initial characterization of a-C:H:Si film

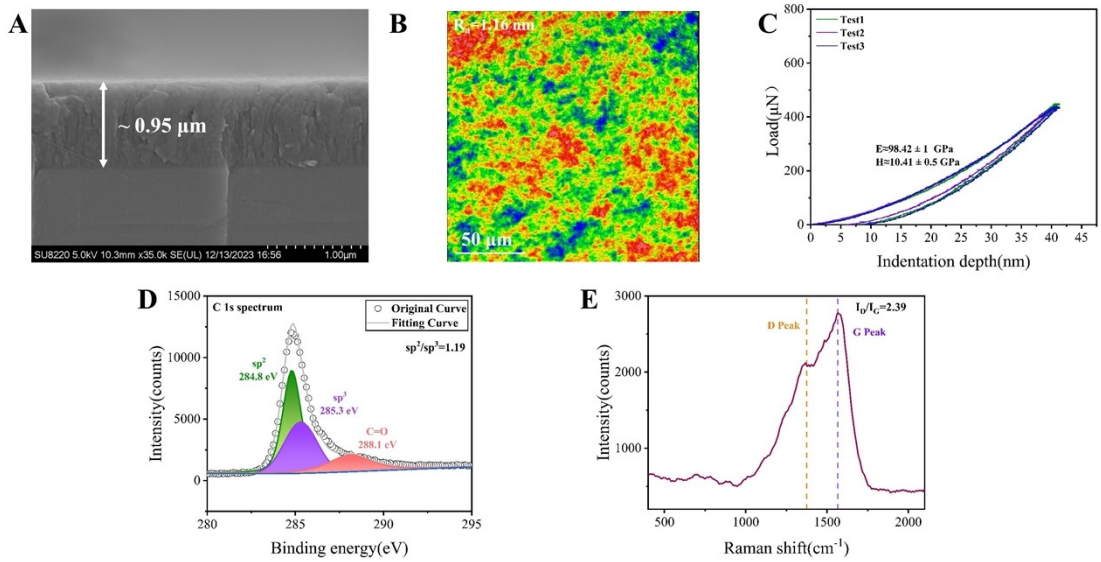

Figure S2. Initial characterization of a-C:H:Si film. (A) SEM result of a-C:H:Si film. (B) Three-dimensional white light interferometry result of a-C:H:Si film. (C) Nanoindentation test of a-C:H:Si film. (D) XPS result of a-C:H:Si film. (E) Raman result of a-C:H:Si film.

4. Friction test on a-C:H:Si film

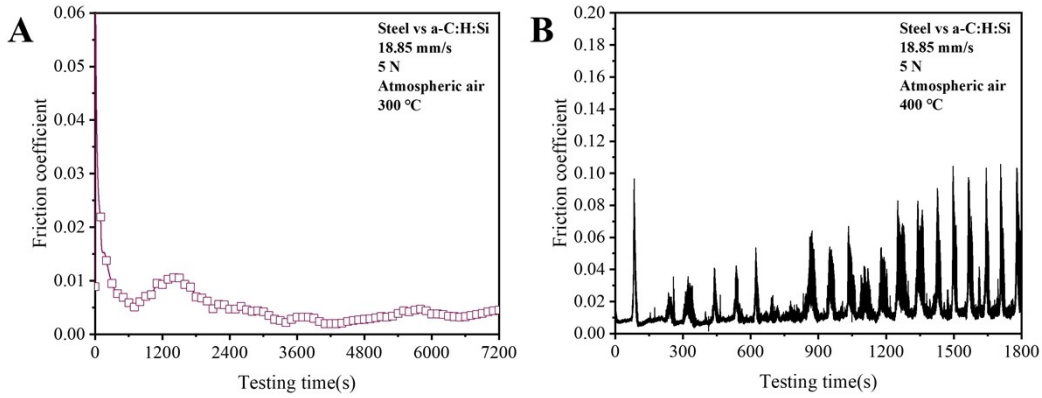

Figure S3. (A) Result of two-hour friction test on steel/a-C:H:Si film in atmospheric air at 300 ℃ (Load was 5 N and sliding speed was 18.85 mm/s). (B) Results of friction tests on steel/ a-C:H:Si film in atmospheric air at 400 ℃.

5. Initial characterization of a-C:H film

The morphology, chemical composition and nano-mechanical properties of the a-C:H film without Si doping were analyzed before the friction tests. The results showed that the thickness of the a-C:H film was about 0.9 μm with the surface roughness of only 0.5 nm (**Figure S4A and S4B**). The Young's modulus was 140.28 ± 3 GPa, and the hardness was 16.42 ± 1 GPa (**Figure S4C**). The results of XPS showed the intensity ratio of sp^2 to sp^3 was 1.35 in the a-C:H film, indicating a high content of sp^2, and the presence of C=O bonding was due to the adsorption of oxygen (**Figure S4D**). Raman spectroscopy showed that the intensity ratio of D to G peaks in the a-C:H film was 2.61 (**Figure S4E**).

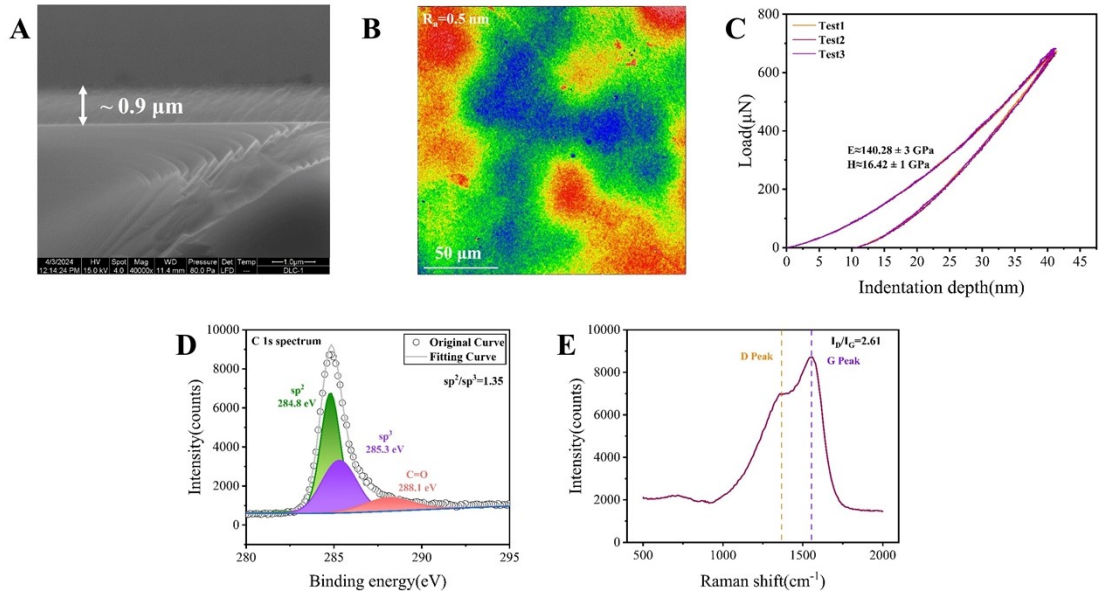

Figure S4. Initial characterization of a-C:H film. (A) SEM result of a-C:H film. (B) Three-dimensional white light interferometry result of a-C:H film. (C) Nanoindentation test of a-C:H film. (D) XPS result of a-C:H film. (E) Raman result of a-C:H film.

6. Friction tests on a-C:H and a-C:H:Si film in different atmosphere

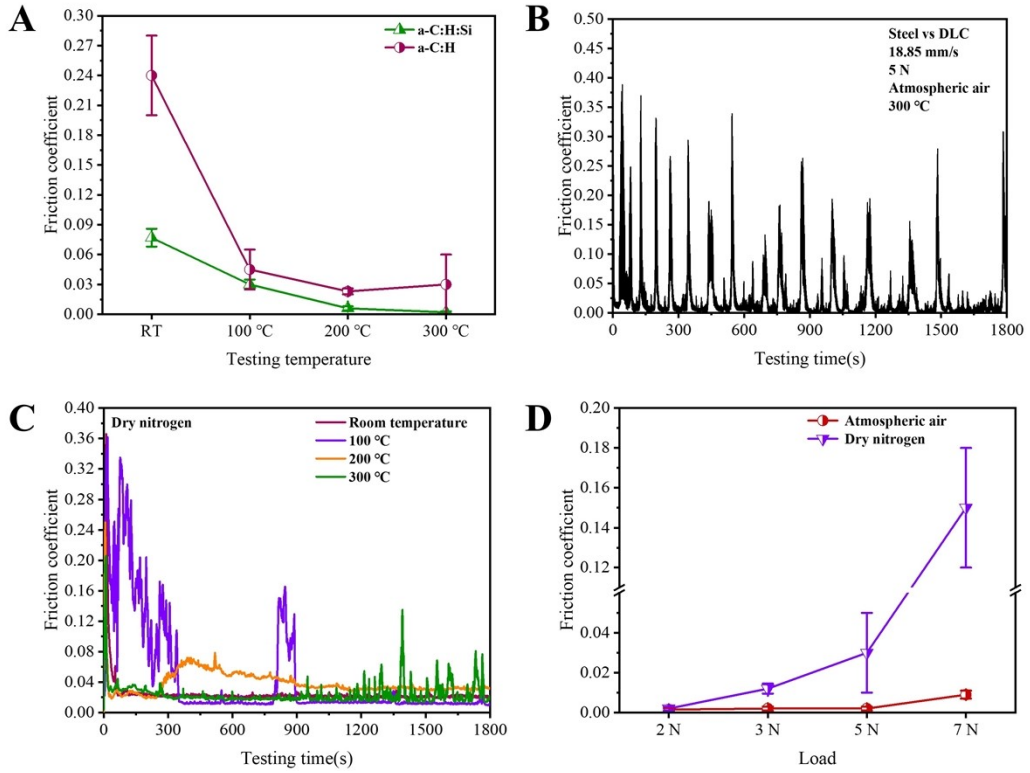

Figure S5. (A) Comparison of results of variable temperature tests on steel/a-C:H:Si film and steel/a-C:H film pairs. (B) Results of friction tests on steel/ a-C:H film pairs at 300 °C. (C) Results of variable temperature friction test on steel/a-C:H:Si film pairs in dry nitrogen (Load was 5 N and sliding speed was 18.81 mm/s). (D) Comparison of results of variable load tests on steel/a-C:H:Si film pairs in atmospheric air and dry nitrogen.

7. Three-dimensional white light interference results of worn region on a-C:H:Si film in atmospheric air and dry nitrogen

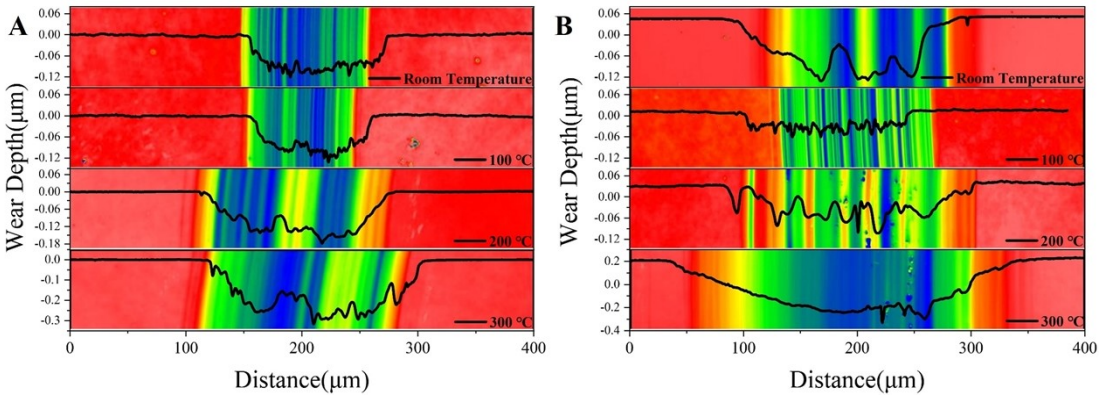

Figure S6. (A) Wear of a-C:H:Si film in atmospheric air at different temperatures. (B) Wear of a-C:H:Si film in dry nitrogen at different temperatures.

8. Results of friction tests with varying oxygen concentration on steel/ a-C:H film pairs at 300 °C

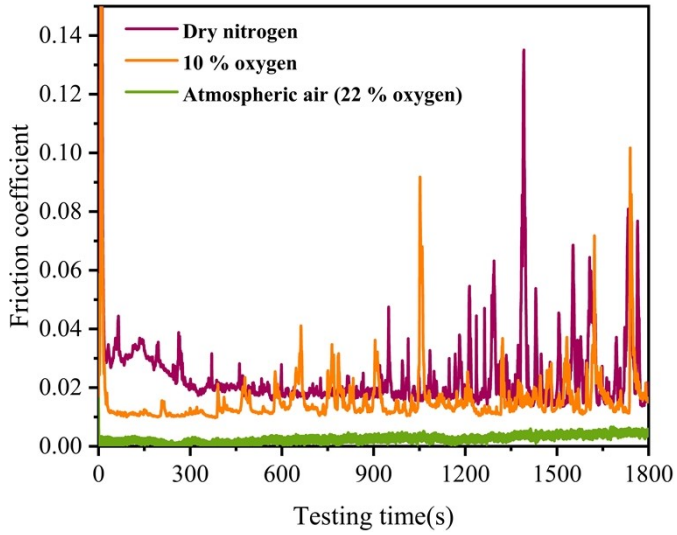

Figure S7. Results of friction tests with varying oxygen concentration on steel/ a-C:H:Si film pairs at 300 ℃.

9. Nanoindentation results in worn region of a-C:H:Si film after friction tests at 300 ℃ and room temperature

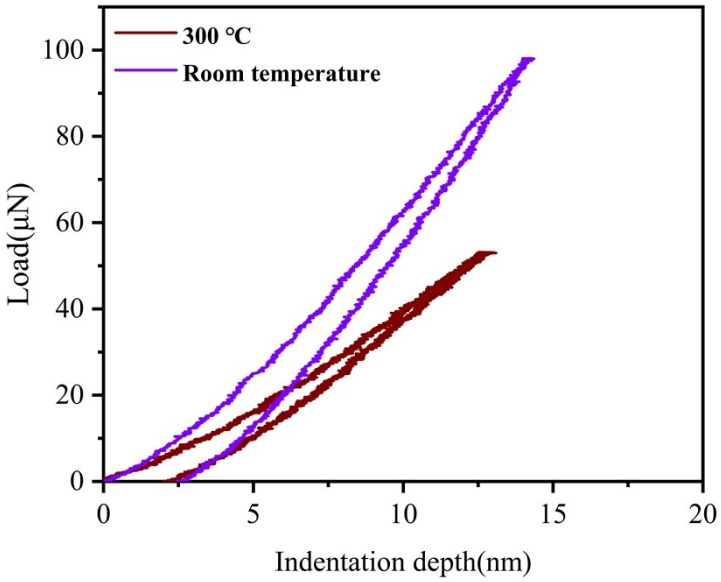

Figure S8. Results of nanoindentation tests on worn region of a-C:H:Si film.

10. SEM and EDS results on the worn region of friction pairs of steel/a-C:H:Si film in atmospheric air at 300 ℃

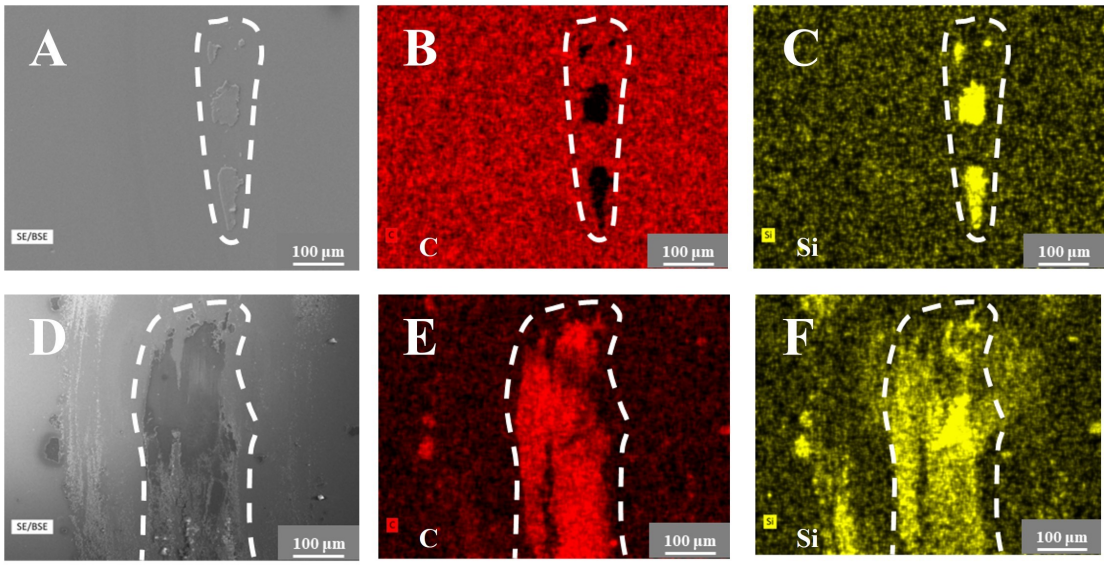

Figure S9. SEM and EDS results in atmospheric air at 300 °C. (A) SEM result on a-C:H:Si film. (B) C spectrum on a-C:H:Si film. (C) Si spectrum on the a-C:H:Si film. (D) SEM result on steel surface. (E) C spectrum on steel surface. (F) Si spectrum on steel surface.

11. SEM and EDS results on the worn region of friction pairs of steel/a-C:H:Si film in atmospheric air at room temperature

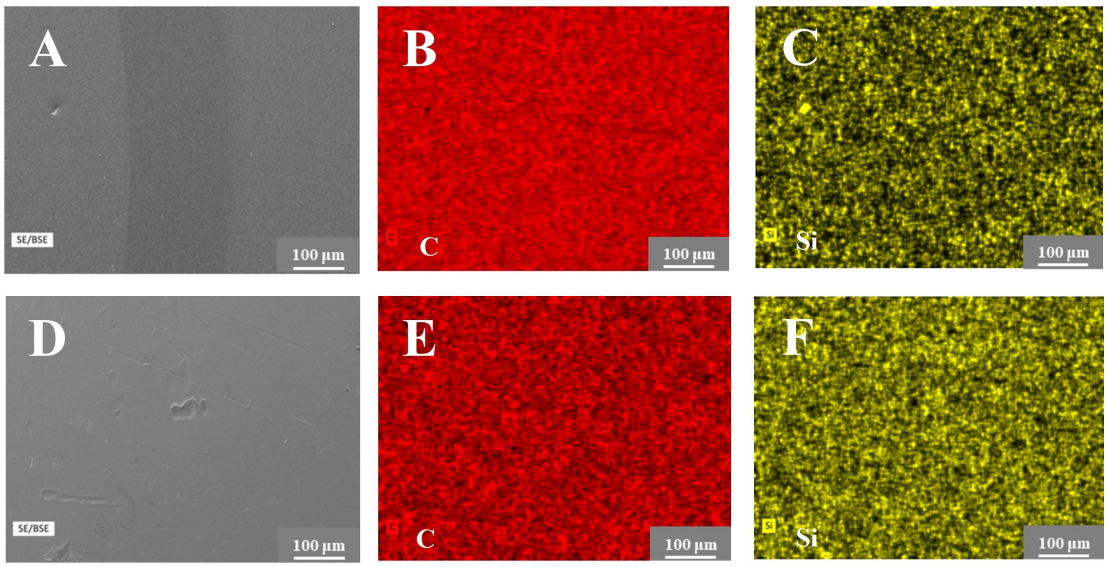

Figure S10. SEM and EDS results under room temperature in atmospheric air. (A) SEM result on a-C:H:Si film. (B) C spectrum on a-C:H:Si film. (C) Si spectrum on the a-C:H:Si film. (D) SEM result on steel surface. (E) C spectrum on steel surface. (F) Si spectrum on steel surface.

12. Raman results on the worn region of friction pairs of steel/a-C:H:Si film in atmospheric air

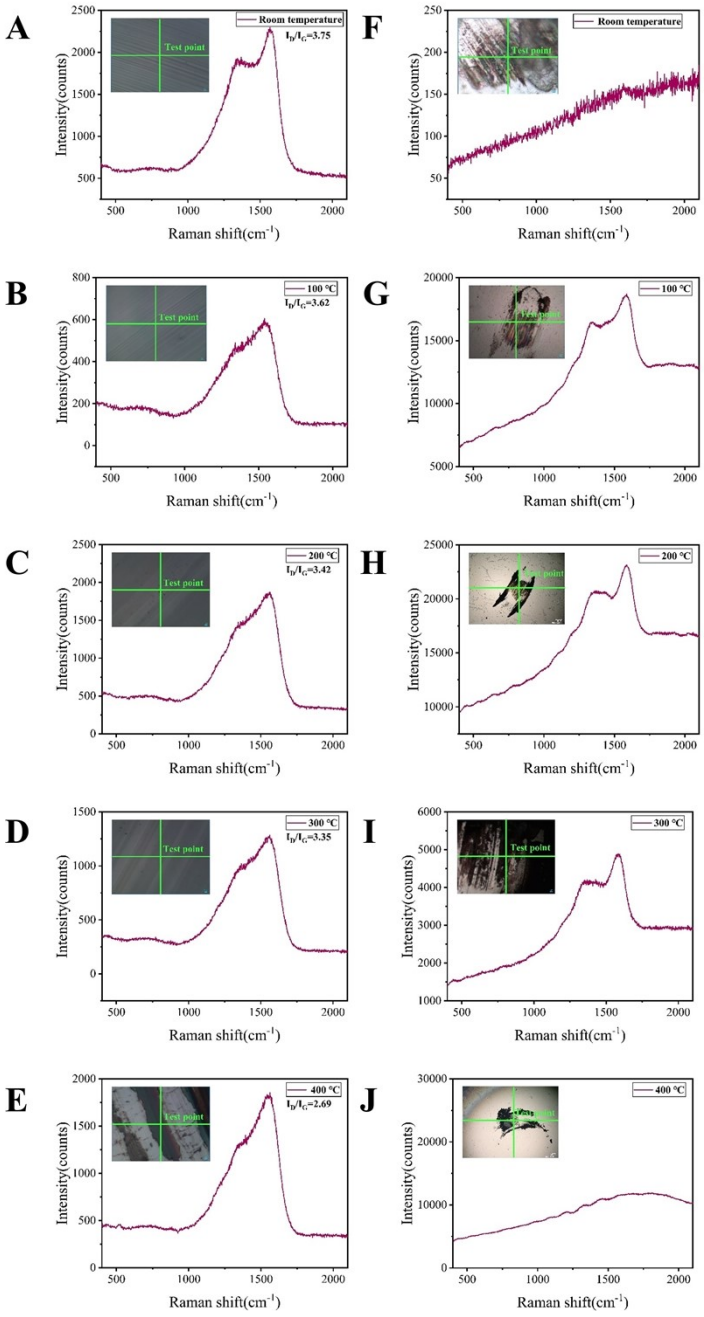

Figure S11. Raman results on worn region of friction pairs in atmospheric air. (A) Raman spectrum in worn track of a-C:H:Si film at room temperature. (B) Raman spectrum in worn track of a-C:H:Si film at 100 ℃. (C) Raman spectrum in worn track of a-C:H:Si film at 200 ℃. (D) Raman spectrum in worn track of a-C:H:Si film at 300 ℃. (E) Raman spectrum in worn track of a-C:H:Si film at 400 ℃. (F) Raman spectrum in worn region of steel surface at room temperature. (G) Raman spectrum in worn region of steel surface at 100 ℃. (H) Raman spectrum in worn region of steel surface at 200 ℃. (I) Raman spectrum in worn region of steel surface at 300 ℃. (J) Raman spectrum in worn region of steel surface at 400 ℃.

13. Relation curves between load and indentation depth

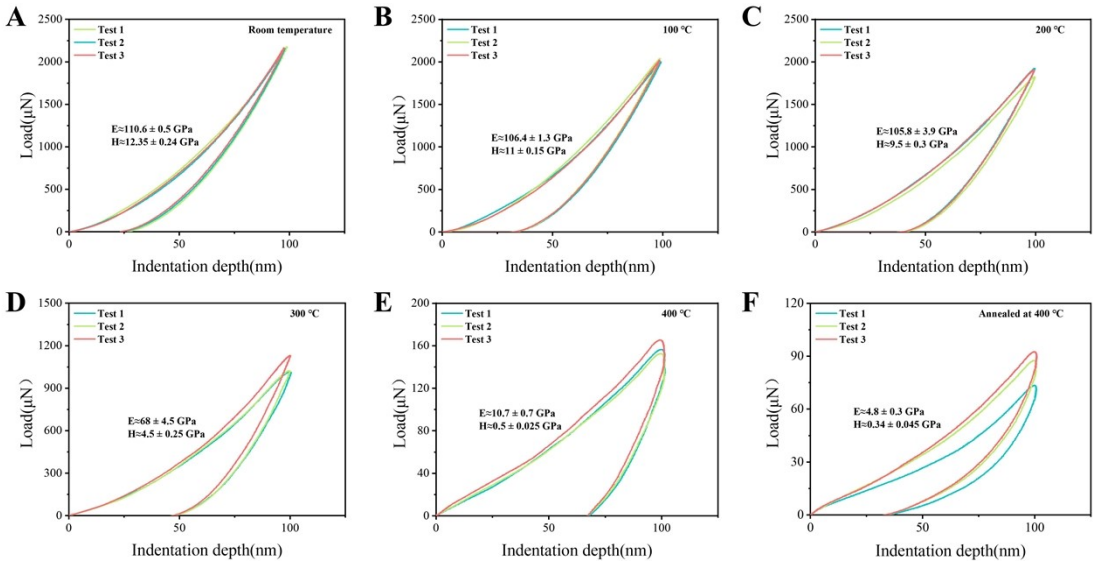

Figure S12. (A) Relation curve between load and indentation depth at room temperature. (B) Relation curve between load and indentation depth at 100 ℃. (C) Relation curve between load and indentation depth at 200 ℃. (D) Relation curve between load and indentation depth at 300 ℃. (E) Relation curve between load and indentation depth at 400 ℃. (F) Relation curve between load and indentation depth after annealing at 400 ℃.

14. Raman spectroscopy and friction tests results of annealed a-C:H:Si film

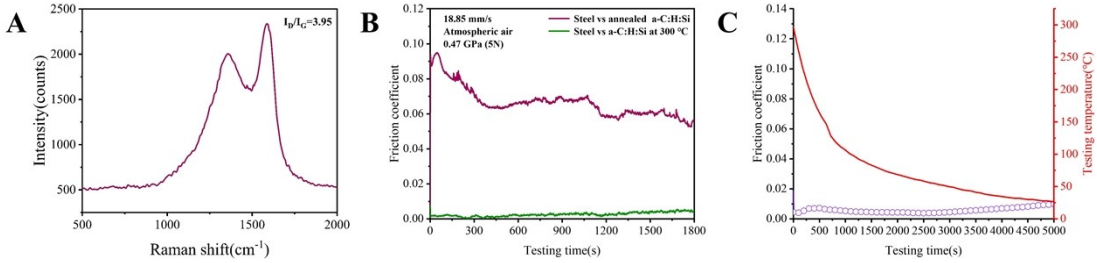

Figure S13. (A) Raman result of a-C:H:Si film after annealing treatment. (B) Friction test results of a-C:H:Si film after annealing treatment. (C) Friction result of a-C:H:Si film when the testing temperature gradually reduced from 300 ℃ to room temperature.

15. Raman results in worn region, unworn region and debris of a-C:H:Si film

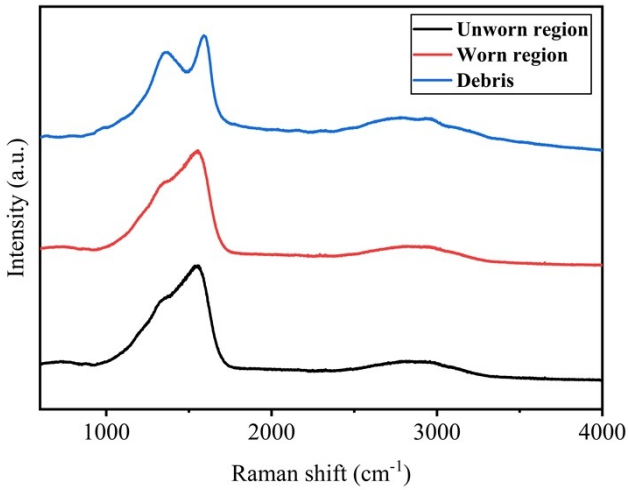

Figure S14. Raman results in a-C:H:Si film after friction tests at 300 ℃

16. TEM and EDS results of tribofilm on steel surface

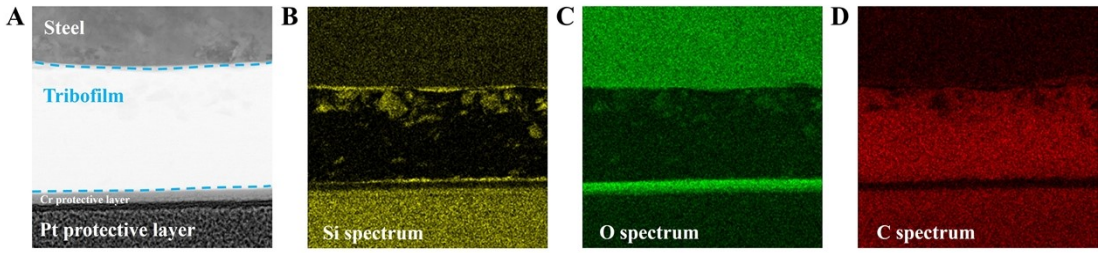

Figure S15. TEM and EDS results on worn region of steel surface. (A) Tribofilm on steel surface. (B) Distribution of silicon in tribofilm. (C) Distribution of oxygen in tribofilm. (D) Distribution of carbon in tribofilm.

17. Enlarged view of TEM results on steel surface after friction tests in dry nitrogen at 300 ℃

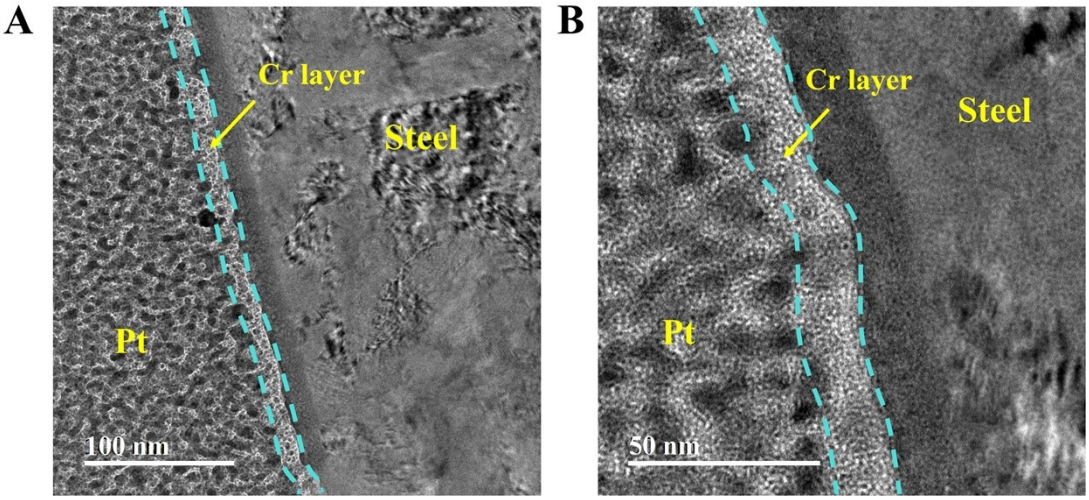

Figure S16. (A) TEM results on steel surface after friction tests in dry nitrogen at 300 ℃ with scale of 100 nm (B) TEM results on steel surface after friction tests in dry nitrogen at 300 ℃ with scale of 50 nm.

18. Models and methodology of molecular dynamics simulations

In this work, classic molecular dynamics (MD) simulations are performed to investigate the oxidation and friction properties of Si-doped diamond from molecular level. To this end, MD box with dimensions of around 64 × 30 × 110 $Å^3$ are created, in which crystalline diamond with dimensions of 64 × 30 × 55 $Å^3$ is placed at the bottom region, whereas at the top region, metallic Fe with a thickness of 30 Å is placed. In the middle region confined by Si-doped diamond and metallic Fe, 500 O2 molecules are randomly inserted. For the diamond, 10% carbon atoms are randomly replaced to create Si-doped diamond, and 20% of the carbon atoms on the surface are terminated by hydrogen atoms. Periodic boundary conditions (PBCs) are imposed in the planar (*x* and *y*) surface directions to mimic large diamond structures, while a wall-boundary condition is applied in the out-of-plane (*z*) direction to avoid the effect of PBC image. To describe the atomic interactions in the diamond systems, the reactive forcefield (ReaxFF) potential is utilized.[1]

Prior to MD simulations, as-generated diamond-based systems are optimized to a local configuration with energy and force tolerances of 1.0 × 10-4 Kcal/mol and 1.0 × 10-4 Kcal/mol·Å, respectively. Soon afterwards, MD simulations are performed to further relax the samples with 100,000 timesteps at temperature of 300 K under NVT (constant number of particles, constant volume, and constant temperature) ensemble, in

which the temperature is controlled by Nose-hoover thermostat. Finally, as-relaxed samples are thermally oxidized at 2000K under NVT (constant number of particles, constant volume, and constant temperature) ensemble. During all MD simulation, carbon and Fe atoms in the bottom region and top regions with thickness of 10 Å are fixed. The atom motions in the diamond-based systems follow the classical Newton's motion, in which the velocity-Verlet algorithm with timestep of 0.25 fs is applied to integrate the classic Newton's equation. All the MD calculations are implemented using the Large-scale Atomic-Molecular Massively Parallel Simulator (LAMMPS) software package.[2]

19. Statistical results of molecular dynamics (MD) simulations

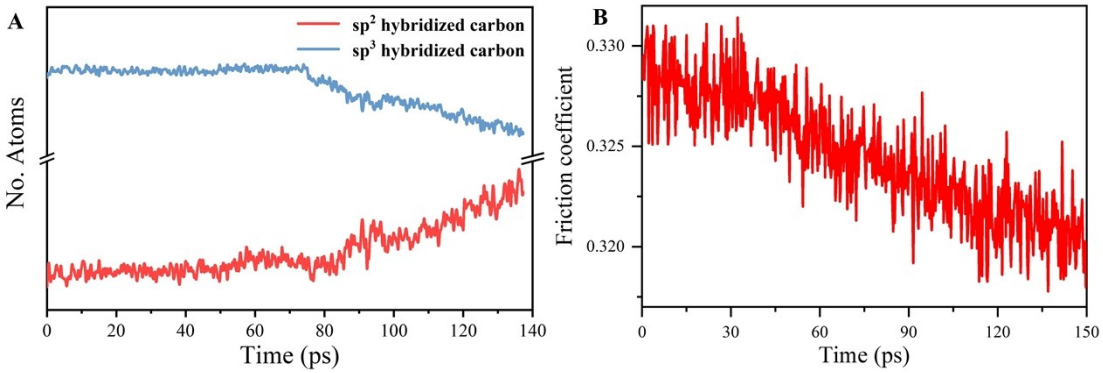

Figure S17. (A) Variation in the number of sp^2 and sp^3 hybridized carbon atoms in running-in period. (B) Variation of friction coefficient with time in running-in period.

20. Summary of existing researches on the tribological properties of diamond-like carbon film in atmospheric air and nitrogen

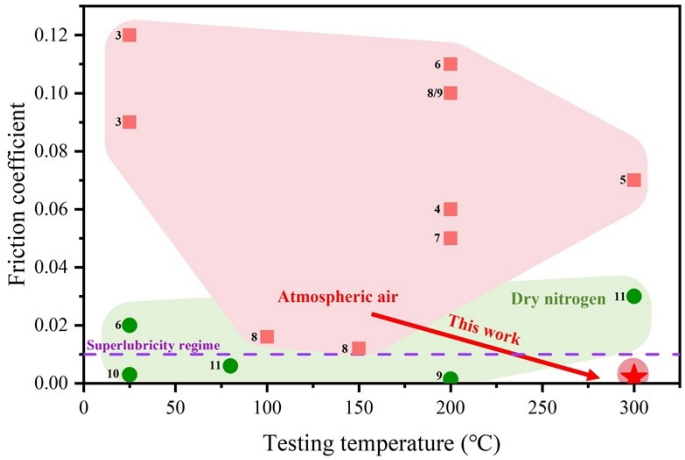

Figure S18. Summary chart of existing studies on tribological properties of diamond-like carbon film

Table S2 Summary table of existing studies on tribological properties of diamond-like carbon film

Friction pairs	Testing temperature	Testing atmosphere	Friction coefficient	Reference
a-C:H/a-C:H	Room temperature	Ambient air	0.12	3
a-C:H/a-C:H	Annealed at 200 °C	Ambient air	0.09	3
Steel/DLC	200 °C	Ambient air	0.06	4
Al_2O_3/Si-DLC	300 °C	Ambient air	0.07	5
Steel/DLC	200 °C	Ambient air	0.11	6
a-C:H/a-Si:O	200 °C	Ambient air	0.05	7
Al_2O_3/DLC	100 °C	Ambient air	0.016	8
Al_2O_3/DLC	150 °C	Ambient air	0.012	8
Al_2O_3/DLC	200 °C	Ambient air	0.1	8
Al_2O_3/Si-DLC	200 °C	Ambient air	0.1	9
H-DLC/H-DLC	Room temperature	Dry nitrogen	0.003	10
Steel/H-DLC	80 °C	Dry nitrogen	0.006	11
Steel/H-DLC	200 °C	Dry nitrogen	0.0015	11

Steel/H-DLC	300 ℃	Dry nitrogen	0.03	11
Steel/DLC	Room temperature	Nitrogen (RH-5%)	0.02	6
Steel/a-C:H:Si	**300 ℃**	**Ambient air**	**0.002**	**This work**

References:

1. Y. Zheng, S. Hong, G. Psofogiannakis, G. B. Rayner, S. Datta, A. C. T. van Duin and R. Engel-Herbert, *ACS Appl. Mater. Interfaces*, 2017, **9**, 15848-15856.
2. S. Plimpton, *J. Comput. Phys.*, 1995, **117**, 1-19.
3. L. Huang, J. Yuan, C. Li, Z. Wang, T. Zhou and Z. Yin, *Vacuum*, 2016, **127**, 96-102.
4. J. Wang, J. Pu, G. Zhang and L. Wang, *Tribology International*, 2015, **81**, 129-138.
5. W. Yu, J. Wang, W. Huang, L. Cui and L. Wang, *Tribology International*, 2020, **146**.
6. H. Li, T. Xu, C. Wang, J. Chen, H. Zhou and H. Liu, *Thin Solid Films*, 2006, **515**, 2153-2160.
7. S. Bhowmick, A. Banerji, M. J. Lukitsch and A. T. Alpas, *Wear*, 2015, **330-331**, 261-271.
8. D. Wang, Z. Gong, B. Jiang, G. Yu, G. Liu and N. Wang, *Diamond and Related Materials*, 2020, **107**.
9. B. Yang, Y. Zheng, B. Zhang, L. Wei and J. Zhang, *Surface and Interface Analysis*, 2012, **44**, 1601-1605.
10. A. Erdemir, *Surface and Coatings Technology*, 2001, **146-147**, 292-297.
11. P. Huang, X. Chen, W. Qi, J. Tian, J. Xu, K. Wang, W. Deng, C. Zhang and J. Luo, *Advanced Functional Materials*, 2024, DOI: 10.1002/adfm.202409503.